The 9th International School on
Beam Dynamics and Accelerator Technology (ISBA26)

19–28 October 2026

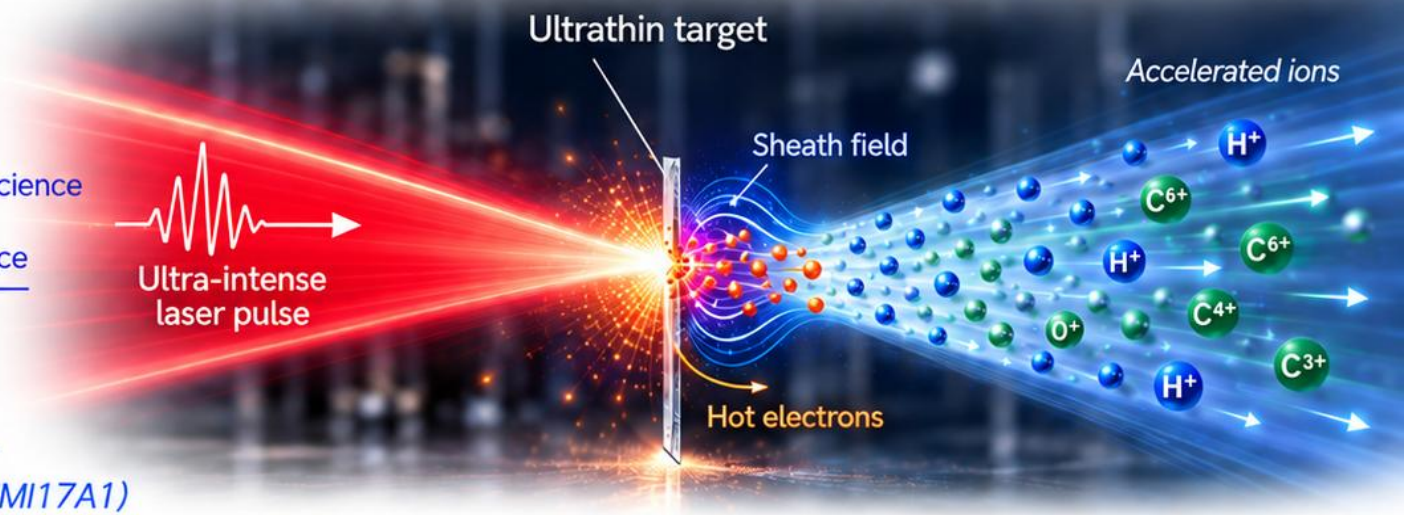
Hiroshima International Plaza,
Higashi-Hiroshima, Japan



Foundation of Laser Ion Acceleration

QST
National Institutes for Quantum Science and Technology (QST)
Kansai Institute for Photon Science

Sadaoki Kojima



This research is supported by the JST-Mirai Program (JPMJMI17A1)

Lecture Roadmap

			Slides
1	Introduction to Laser-Driven Ion Acceleration	Motivation, basic concepts, and comparison with conventional accelerators	3–5
2	Laser–Plasma Interaction	Plasma formation, critical density, and electromagnetic wave propagation in plasmas	6–12
3	Laser Energy Absorption and Fast-Electron Generation	Single-electron motion, absorption mechanisms, and fast-electron generation	13–22
4	Fast-Electron Transport and Sheath Formation	Transport of fast-electron currents in solid targets and formation of rear-surface sheath fields	23–28
5	Target Normal Sheath Acceleration (TNSA)	Plasma expansion models, TNSA beam characteristics, and recent experimental progress	29–37
6	Summary	Review of the lecture and key takeaways	38–39

POINT **Laser–plasma interactions transfer laser energy to charged particles through different ion acceleration mechanisms.**

Section 1

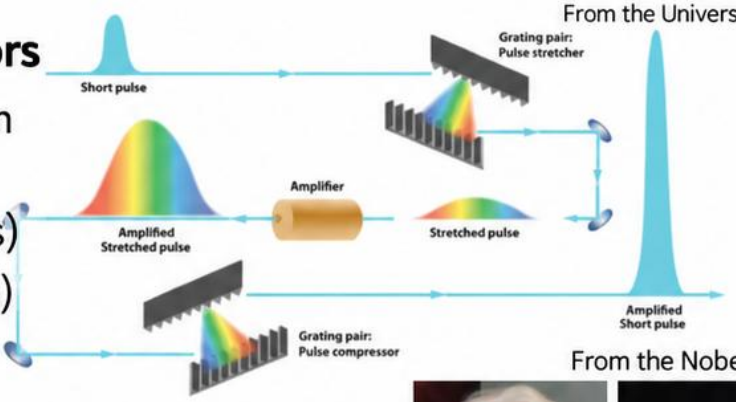
Introduction to Laser-Driven Ion Acceleration

Fusion of Accelerator Science and Laser Science

Challenges of Conventional Accelerators

- Driving high-energy physics and synchrotron radiation science
- Large scale (hundreds of meters to kilometers)
- High cost (tens to hundreds of billions of yen)
- Miniaturization and cost reduction are strong social demands

From the University of Michigan website



From the Nobel Foundation website





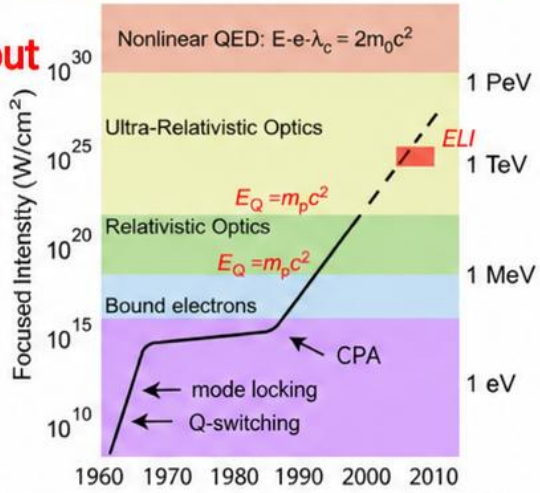
Innovation in Laser Science

- 1985: Chirped Pulse Amplification (CPA) was invented

D. Strickland and G. Mourou: Opt. Commun. 56, 219 (1985).

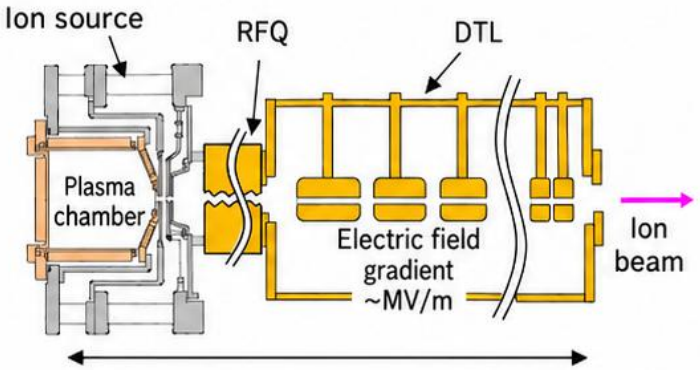
POINT Tabletop-scale laser systems can reach petawatt-class output

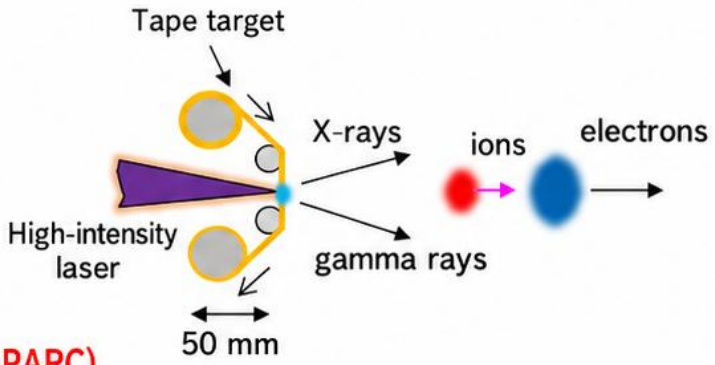
- High-intensity laser: $I > 10^{18}$ W/cm^2 → electrons undergo relativistic motion
- Acceleration gradient: TV/m (10,000 times higher than conventional accelerators)
- Two major streams
  1. Electron acceleration → electrons are accelerated to GeV energies by plasma waves (cm scale)
  2. Ion acceleration → strong electric fields generated in high-density plasma accelerate ions



Plasma Phys. Control. Fusion 49 (2007) B667–B675

Comparison of RF Accelerators and Laser Accelerators





For proton acceleration to 50 MeV, the length is about 30 m (J-PARC)

Item	RF Accelerator	Laser Accelerator
Acceleration principle	Linear interaction between RF electric fields in accelerating cavities and charged particles (electrons or ions)	Nonlinear interaction between an ultrashort-pulse laser and plasma
Interaction scale	Frequency: tens of MHz to tens of GHz Space: m-km (accelerator length)	Frequency: hundreds of THz (laser field) (800 nm wavelength → 375 THz) Space: um-mm (focal region length)
Interaction	Particle-RF field, particle-particle, particle-matter (residual gas, walls)	Laser electromagnetic field-plasma, plasma-generated electromagnetic fields-plasma

POINT **Understanding laser acceleration requires laser-plasma interaction**

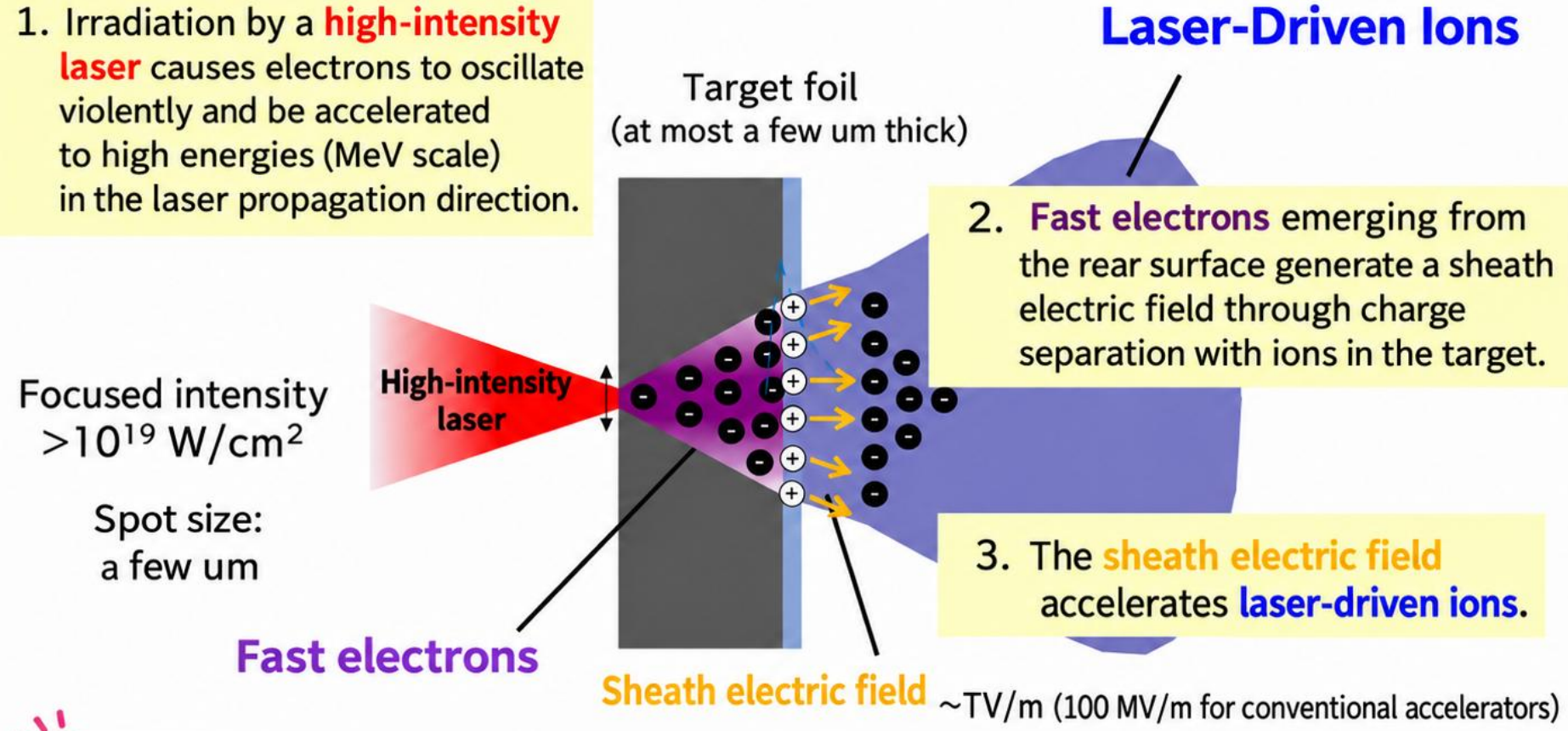
Section 2

Laser–Plasma Interaction

What is Laser-Driven Ion Acceleration? (Basic Mechanism)

Target Normal Sheath Acceleration (TNSA)

1. Irradiation by a **high-intensity laser** causes electrons to oscillate violently and be accelerated to high energies (MeV scale) in the laser propagation direction.



POINT

Let us understand in detail the physical phenomena behind laser-driven ion acceleration.

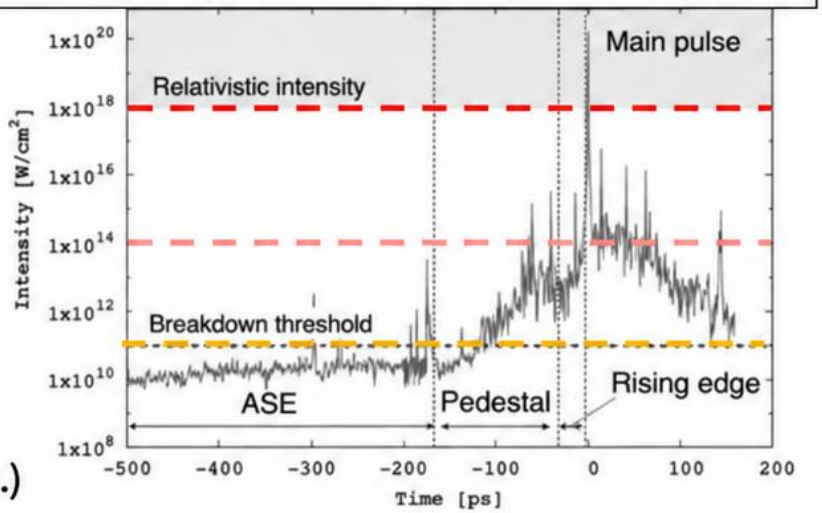
Plasma Formation of a Solid Target

10^{11}~10^{12} W/cm^2
→ multiphoton ionization of outer-shell electrons becomes significant

10^{14}~10^{15} W/cm^2
→ tunnel ionization becomes dominant, and the solid surface is immediately ionized into plasma

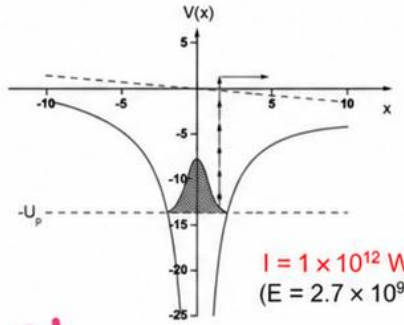
10^{18} W/cm^2
→ electrons oscillate relativistically in the light field
(This regime is called the relativistic intensity regime.)

Temporal intensity structure of a high-intensity laser



Multiphoton Ionization

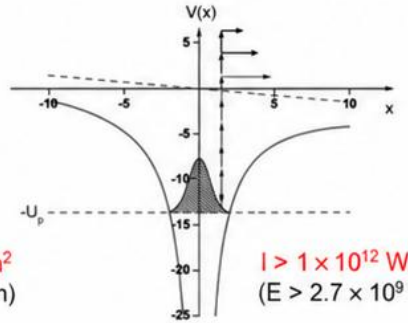
(a) *Multi-Photon Ionization*



I = 1 × 10^{12} W/cm^2
(E = 2.7 × 10^9 V/m)

Above-Threshold Ionization

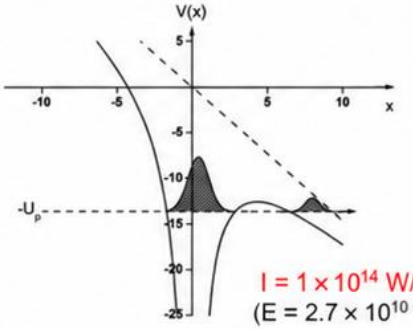
(b) *Above Threshold Ionization*



I > 1 × 10^{12} W/cm^2
(E > 2.7 × 10^9 V/m)

Tunnel Ionization

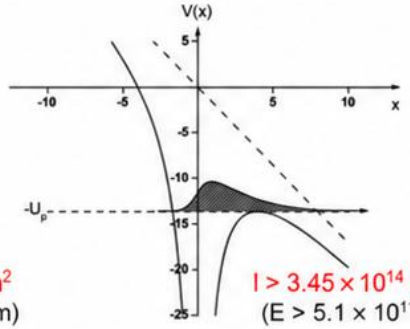
(c) *Tunneling Ionization*



I = 1 × 10^{14} W/cm^2
(E = 2.7 × 10^{10} V/m)

Barrier-Suppression Ionization

(d) *Barrier Suppression Ionization*

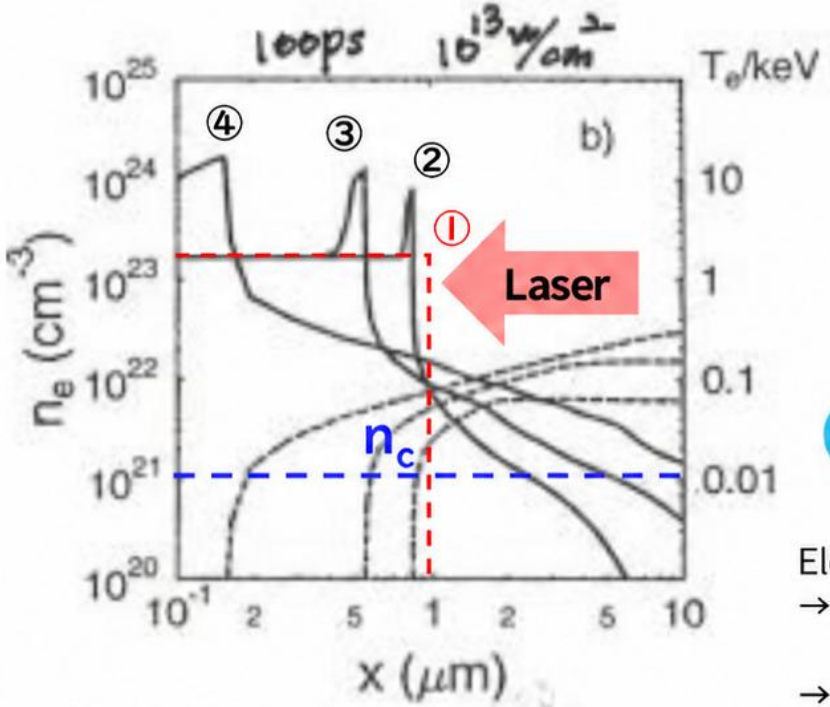


I > 3.45 × 10^{14} W/cm^2
(E > 5.1 × 10^{11} V/m)

POINT

In accelerator science, **impact ionization by electrons driven by RF fields** is dominant.
In laser acceleration, **photoionization by the powerful laser electromagnetic field,** comparable to the atomic binding field, is dominant.

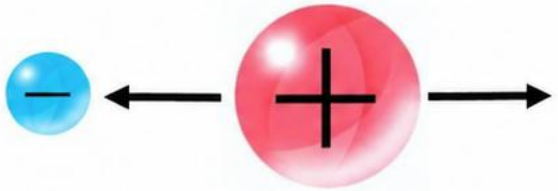
Plasma Expansion and Critical Density



Short Pulse Laser Interactions with Matter
by Dr. Paul Gibbon

The heated plasma begins to expand
→ in front of the solid-density plasma (10^{23} electrons/cm^3), a low-density plasma region is formed.

Interaction between this low-density plasma and the laser is important.



Plasma frequency

$$\omega_p = \sqrt{\frac{n_e e^2}{\varepsilon_0 m_e}}$$

Electrons are displaced relative to ions
→ the centers of positive and negative charge are shifted, generating an electric field
→ this electric field acts as a restoring force pulling electrons back to their original positions
→ electrons undergo **plasma oscillation** due to this restoring force

The higher the plasma density, the higher the plasma frequency
→ the external field (laser field) is cancelled by plasma oscillation

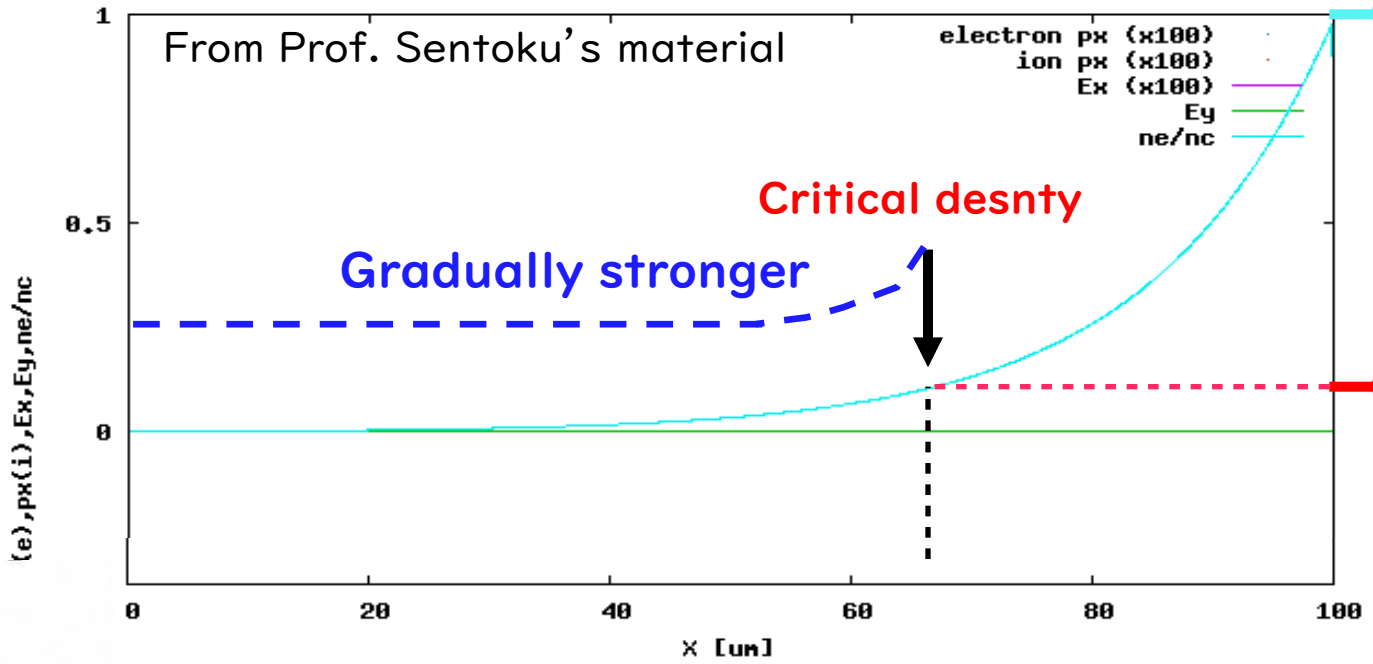
POINT

Density at which the laser frequency equals the plasma frequency
Critical density

$$n_c = \frac{\epsilon_0 m_e \omega^2}{e^2} \approx 1.1 \times 10^{21} \frac{1}{\lambda_{\mu m}^2} \ \mathrm{cm}^{-3}$$

Propagation of Laser Electromagnetic Fields in Plasma

1D Particle-in-Cell simulation



Solid density

10^{23} electrons/cm^3

Critical density

10^{21} electrons/cm^3

- $n_e < n_c$ (Under critical density)

The laser is transmitted and can propagate as a wave inside the plasma.

Resonance absorption and inverse bremsstrahlung absorption occur.

- $n_e > n_c$ (Over critical density)

The laser is reflected and cannot penetrate.

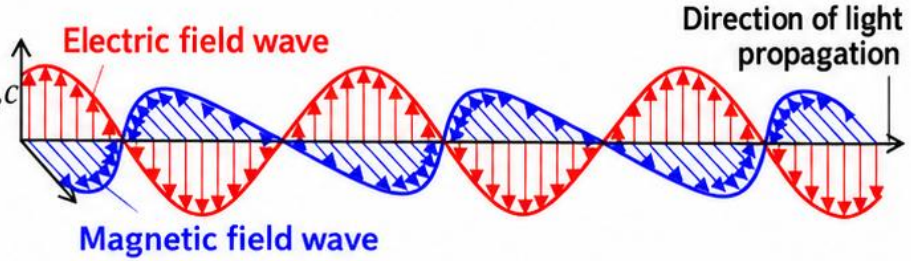
However, with **relativistic effects** it can penetrate up to **gamma n_c**.

Normalized Vector Potential and Relativistic Intensity

How strong must the laser intensity be for relativistic effects to appear?

The oscillatory momentum of an electron in an electromagnetic wave (plane wave) is $p_{osc} = \frac{eE}{\omega}$

Dividing this momentum by the momentum at the speed of light, $m_e c$



Normalized Vector Potential

$$a_0 = \frac{eE}{m_e c \omega} \approx 0.85 \sqrt{I_{18} \lambda^2{}_{\mu m}}$$ is used

E:	laser electric field strength
ω:	laser angular frequency
m_e, e, c:	electron mass, charge, speed of light
$\lambda_{\mu m}$:	laser wavelength [μm]
I^{18}:	laser intensity normalized by 10^{18} W/cm^2

10^{19} [W/cm^2] ⇒ $a_0 = 2.15$
10^{20} [W/cm^2] ⇒ $a_0 = 6.8$
10^{21} [W/cm^2] ⇒ $a_0 = 21.5$
10^{22} [W/cm^2] ⇒ $a_0 = 68$
10^{23} [W/cm^2] ⇒ $a_0 = 215$

POINT

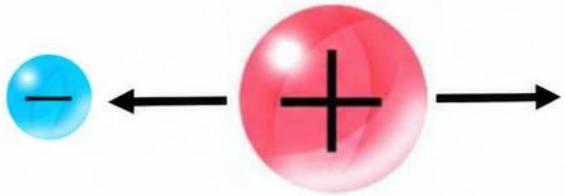
$a_0 \ll 1$: electrons undergo non-relativistic motion (classical oscillation)

$a_0 \gtrsim 1$: electrons oscillate close to the speed of light ⇒ relativistic effects are important

For example, when the laser wavelength is 1 μm, $a_0 \approx 1$
the laser intensity is 1.4×10^{18} [W/cm^2]

Normalized Vector Potential and Relativistic Critical Density (γn_c)

QST



Plasma Frequency

$$\omega_p = \sqrt{\frac{n_e e^2}{\varepsilon_0 m_e}}$$

In a laser electric field, electrons oscillate around ions

The density at which the laser frequency and plasma frequency are equal

Critical Density

$$n_e = \frac{\varepsilon_0 m_e \omega^2}{e^2} \approx 1.1 \times 10^{21} \frac{1}{\lambda_{\mu m}^2} \ \mathrm{cm}^{-3}$$

Critical density is determined only by the laser wavelength (frequency) and does not depend directly on intensity

How does the relativistic effect influence the plasma density through which a laser can propagate?

At high laser intensity, electrons become heavier due to relativistic effects $\langle\gamma\rangle \approx \sqrt{1 + \frac{a_0^2}{2}}$

Relativistic critical density

$$n_{c,\mathrm{eff}} = \gamma n_c$$

10^{19} [W/cm^2]	$\Rightarrow a_0 = 2.15$	$\Rightarrow \gamma = 1.8$
10^{20} [W/cm^2]	$\Rightarrow a_0 = 6.8$	$\Rightarrow \gamma = 4.5$
10^{21} [W/cm^2]	$\Rightarrow a_0 = 21.5$	$\Rightarrow \gamma = 14$
10^{22} [W/cm^2]	$\Rightarrow a_0 = 68$	$\Rightarrow \gamma = 43$
10^{23} [W/cm^2]	$\Rightarrow a_0 = 215$	$\Rightarrow \gamma = 137$

It can reach up to 100 n_c

10^{23} electrons/cc is close to solid density

Section 3

Laser Energy Absorption and Fast-Electron Generation

Single-Electron Motion in a Laser Electromagnetic Field

Equation of Motion for an Electron in a Laser Field

When an electron (charge $-e$, mass m_e) is acted on by the laser electromagnetic field (electric field **E**, magnetic field **B**), its motion follows the Lorentz force.

$$\gamma\, m_e \frac{d\mathbf{v}}{dt} = -e\,(\mathbf{E} + \mathbf{v} \times \mathbf{B}) \qquad \gamma = \frac{1}{\sqrt{1 - v^2/c^2}}$$

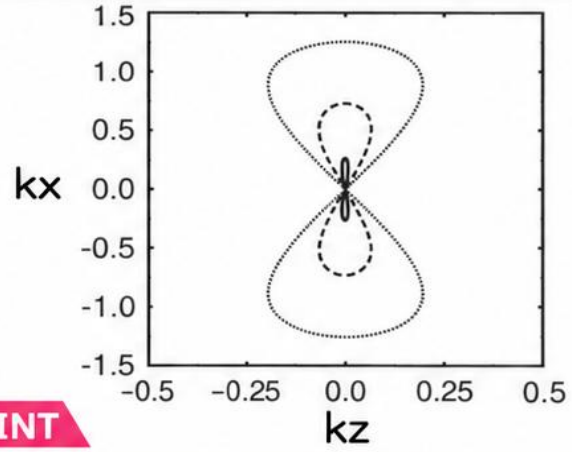
Here, the laser electromagnetic wave is assumed to be a plane wave

$$\mathbf{E}(z,t) = E_0 \cos(kz - \omega t)\,\hat{\mathbf{x}}, \qquad \mathbf{B}(z,t) = \frac{E_0}{c}\cos(kz - \omega t)\,\hat{\mathbf{y}}$$

∗ The magnetic-force term (second term) is extremely weak compared with the electric-force term (first term)

The electron oscillates in the x direction due to the electric field, and simultaneously oscillates in the z direction with twice the period due to the magnetic field

Low-Intensity Laser (non-relativistic, $a_0 \ll 1$)

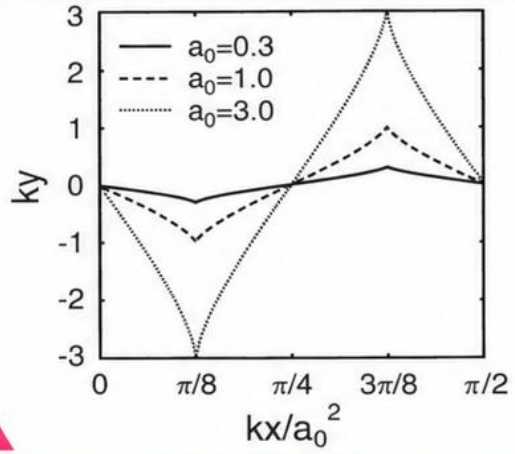


POINT

The electron trajectory traces a figure-eight

∗ Even at high intensity, in the inertial frame moving with the average drift velocity

High-Intensity Laser (relativistic, $a_0 \geq 1$)



POINT

Viewed in the laboratory frame, the electron drifts in the z direction (laser propagation direction)

Single-Electron Motion in a Laser Electromagnetic Field (Plane Wave)

QST

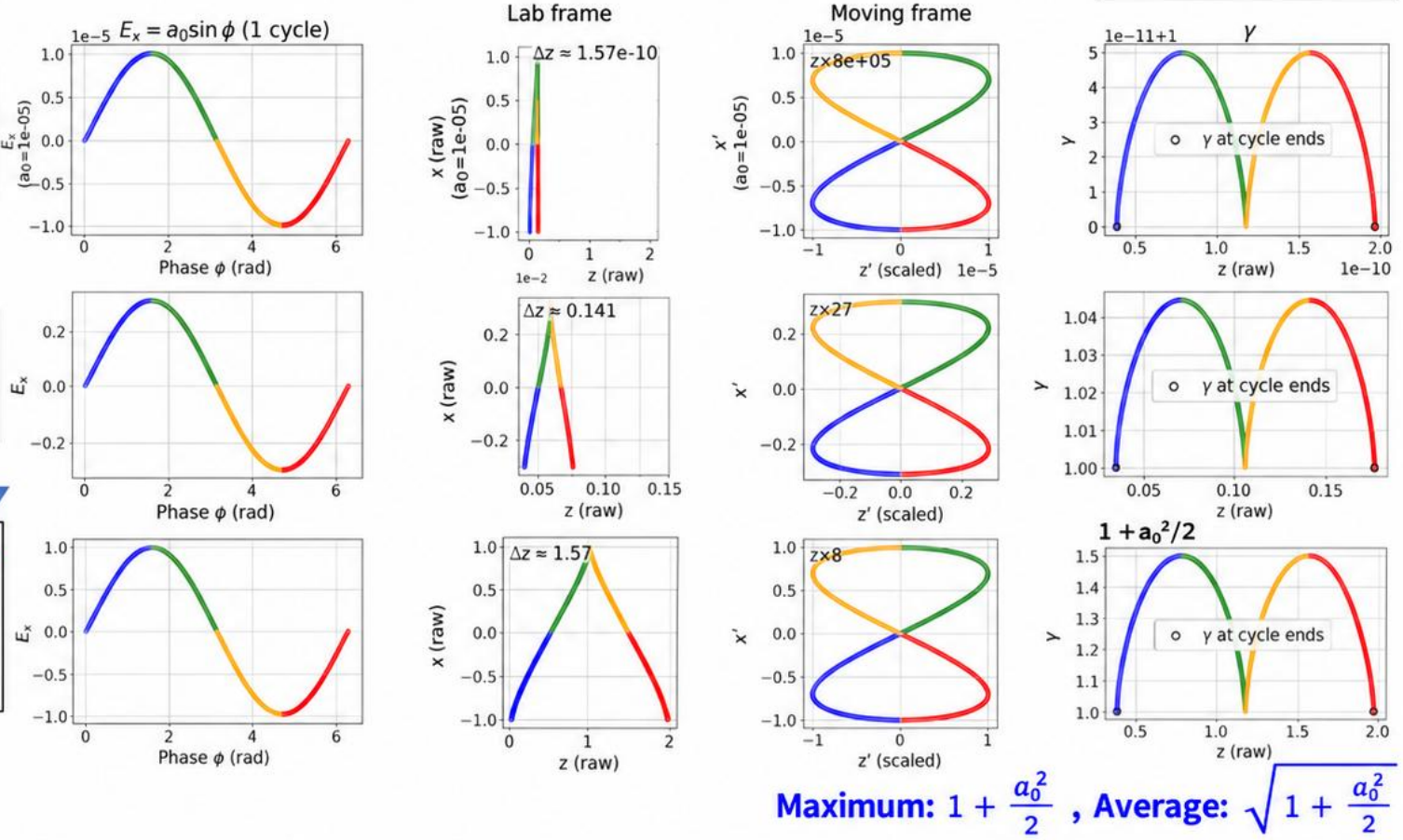
Low-Intensity Laser
$(a_0 \ll 1)$

$a_0 = 0.3$
$(10^{17}\ \mathrm{W/cm^2})$

High-Intensity Laser
$a_0 = 1$
$(10^{18}\ \mathrm{W/cm^2})$

POINT

Laser electric field	Laboratory frame	Inertial frame moving with the drift velocity	Lorentz factor (energy)



Maximum: $1 + \frac{a_0^2}{2}$, **Average:** $\sqrt{1 + \frac{a_0^2}{2}}$

- In the inertial frame, at any intensity, the electron moves in a figure-eight
- It drifts, but after one cycle the velocity returns to zero (it is not accelerated)

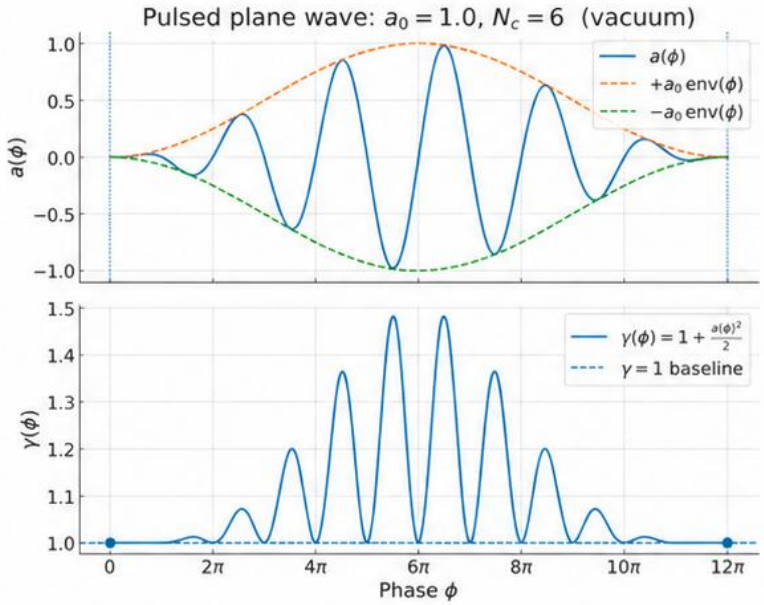


Electron Acceleration by Laser Electromagnetic Fields

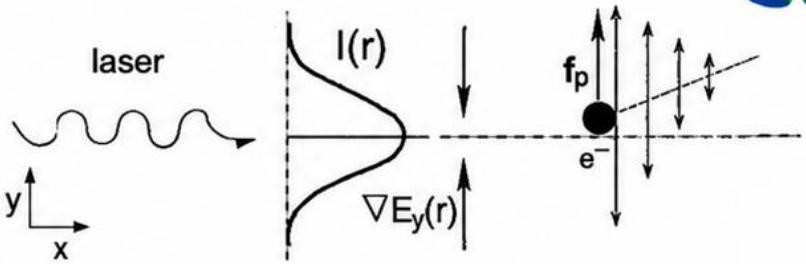
Under the assumptions so far, vacuum × infinite plane wave ⇒ no net energy gain (no acceleration)

In reality, how do electrons obtain a net energy gain?

Pulse? (temporal variation)



Focusing? (spatial variation)



They only drift from the stronger region (center) to the weaker region (outer side)

⇒ ponderomotive force

In either case, the net energy gain is zero (cannot accelerate)

POINT

Assumptions so far: vacuum × infinite plane wave × single electron These conditions were also assumed

+ (no boundary condition, no static field, electrons enter from outside the field and leave again)

Electron Acceleration by Laser Electromagnetic Fields

- No boundary condition ⇒ irradiate the laser onto plasma (boundary condition)
- No static field ⇒ electrostatic and magnetostatic fields are generated by plasma expansion
- Electrons enter from outside the field and leave ⇒ electrons are generated by ionization, and escape through collisions

Depending on the plasma state and laser focusing intensity, various absorption, heating, and electron-acceleration mechanisms have been reported

Mechanism	Main location / condition	Dominant factor	Energy absorption mode	Characteristics of generated electrons
Inverse Bremsstrahlung (collisional absorption, classical absorption)	Underdense region	Collision frequency	Heating due to collisions between laser-driven electrons and plasma particles	Low-energy thermal distribution (keV)
Resonance absorption	Pre-plasma, oblique incidence	P polarization, density-gradient scale length	The p-polarized component excites plasma waves and transfers energy to electrons	Tens-of-keV fast electrons
Vacuum heating (Brunel absorption)	Sharp density gradient	P polarization, sharp gradient	Electrons are pulled out toward the vacuum side by the laser electric field and then reinjected (pushed back in)	Tens-of-keV fast electrons
J×B heating (ponderomotive heating)	Relativistic intensity ($a_0 \gtrsim 1$)	v×B force	Drift in the laser propagation direction due to the v×B force	MeV-order fast electrons

POINT

- $< 10^{17}$ W/cm^2 : inverse bremsstrahlung dominates (but weak for fs)
- 10^{17}–10^{18} W/cm^2 : resonance absorption or vacuum heating dominates
- $\gtrsim 2\times10^{18}$ ($a_0 \gtrsim 1$) W/cm^2 : J×B heating dominates

Inverse Bremsstrahlung

Mechanism

Electrons oscillating in the laser electric field **absorb energy through collisions** with ions and other electrons, **and it is accumulated in the plasma as heat**

Conditions

- **High-density, low-temperature plasma** (collision frequency ν is sufficiently large)
- **Below critical density** (underdense region)
- **Effective for ns-class long-pulse lasers**
- Relatively low intensity ($<10^{17}$ W/cm^2)

$$\nu_{ei} \approx \frac{4\sqrt{2\pi}}{3} \frac{Z n_i e^4 \ln \Lambda}{(4\pi\epsilon_0)^2 m_e^{1/2} (k_B T_e)^{3/2}}$$

Characteristics

- The entire plasma is **heated thermally**
- Fast-electron generation is weak

Trend

- As the wavelength becomes shorter, the **absorption rate increases** (density ↑)
- As the intensity increases, the **absorption rate decreases** (temperature ↑)

As the plasma temperature rises, the collision frequency decreases

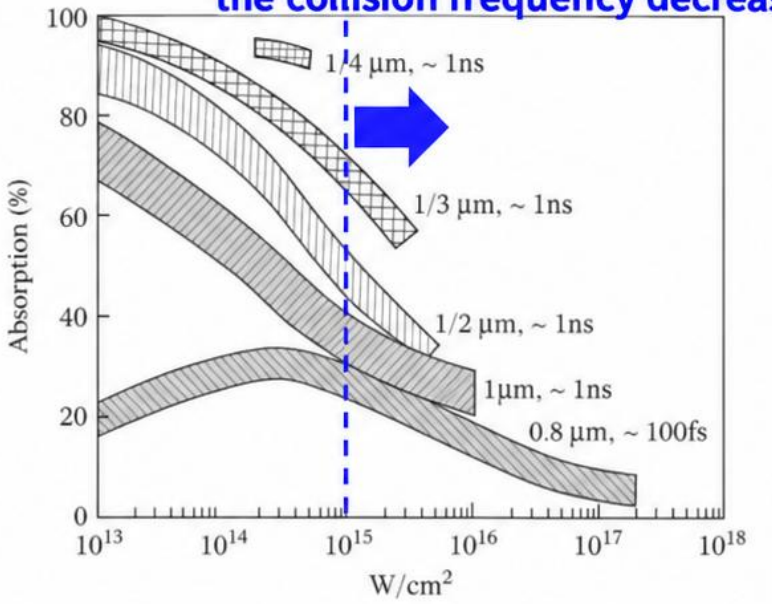


Figure taken from Eliezer, *An introduction to intertial confinement fusion* (2002).

D. W. Forslund and J. P. Freidberg, Phys. Rev. Lett. 27, 1189 (1971).

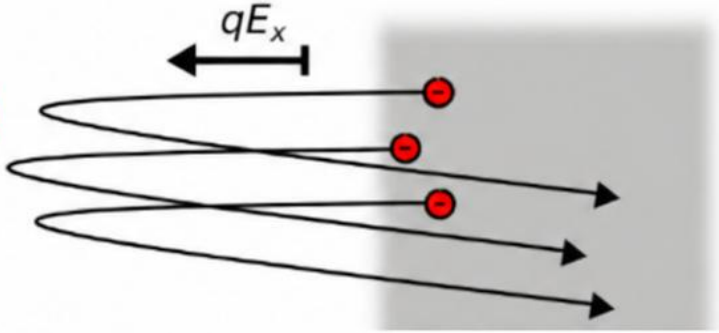
Vacuum Heating (Brunel Absorption)

Mechanism

Electrons are **pulled out** from the plasma surface into the vacuum by the laser electric field, and are **pushed back** into the plasma during the next half cycle. Through this back-and-forth motion, the electrons directly gain energy from the laser electric field, and high-energy electrons are injected into the plasma.

Conditions

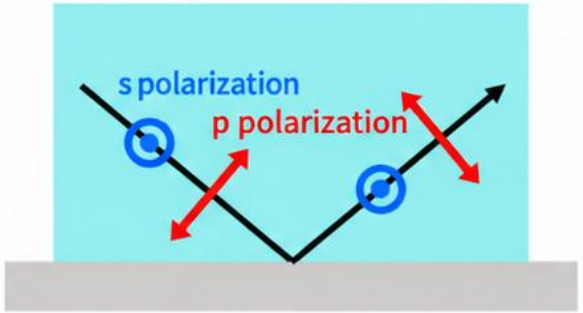
- **Steep plasma density gradient (scale length $L \ll \lambda$)**
- **p-polarized laser and oblique incidence**
- High-intensity fs–ps laser (10^{16}–10^{18} W/cm^2)



Laser-driven Ion Acceleration
Intensive School Laser, Plasma & Fusion
Rethymnon, Crete, Greece, 3 September 2024

Characteristics

- Nonlinear absorption with high efficiency
- Absorption efficiency depends on incidence angle and polarization (especially maximum around 45°)
- **The generated electrons are non-thermal and fast, and can readily serve as the electron source for TNSA**
- If the prepulse is strong, pre-expansion makes resonance absorption or inverse bremsstrahlung dominant



Brunel effect (F. Brunel, Phys. Rev. Lett., 59, 52 (1987))

Resonance Absorption

Mechanism

When laser light is reflected at the critical-density surface, the electric-field component of p-polarized light at oblique incidence excites electron plasma waves, and **the laser energy is strongly absorbed locally.**

Conditions

- p polarization, oblique incidence, and a moderate density gradient
- $(L/\lambda \approx 0.1\text{–}1)$
- Moderate intensity $(10^{17}\text{–}10^{18}\ \mathrm{W/cm^2})$

Characteristics

- Generates high-energy electrons near the critical density

Angle dependence

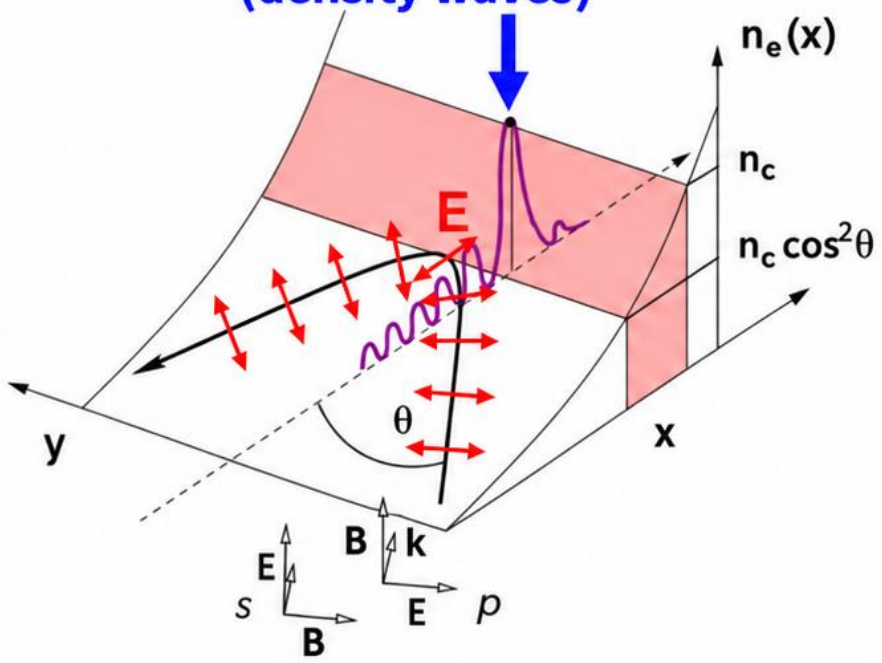
- **Moderate incidence angle (around 20–30°)**
- **The longitudinal field component becomes large and efficiently excites plasma waves**

→ The absorption efficiency becomes maximum

What is resonating?

Plasma frequency = laser frequency

Resonant excitation of plasma waves (density waves)



J. P. Freidberg, R. W. Mitchell, R. L. Morse, and L. I. Rudsinski, Phys. Rev. Lett. 28, 795 (1972).

J×B Heating (Ponderomotive Heating, v×B Force)

Mechanism

At relativistic intensity, the **laser magnetic field** can no longer be neglected.
While electrons oscillate transversely due to the electric field, they are **drift-accelerated** in the **laser propagation direction** by the **v×B force**.

Conditions

- $a_0 \gtrsim 1$ ($I \gtrsim 2 \times 10^{18}$ W/cm² @ 800 nm)
- Independent of polarization and incidence angle
- Operates universally in the relativistic intensity regime

$$\gamma m_e \frac{d\mathbf{v}}{dt} = -e\left(\mathbf{E} + \mathbf{v} \times \mathbf{B}\right)$$

Effective even at low intensity

More effective at high intensity

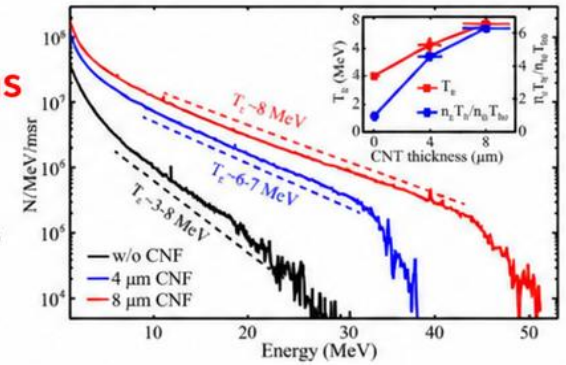
Characteristics

- Accelerates directional MeV electrons along the laser propagation direction
- Dominant in the ultra-relativistic regime
- No energy dissipation due to collisions
- The energy distribution of accelerated electrons is exponential

$$\exp(-E/T_e)$$

- The typical slope temperature of the obtained electrons is

$$T_e = m_e c^2 \left(\sqrt{1 + a_0^2} - 1\right)$$



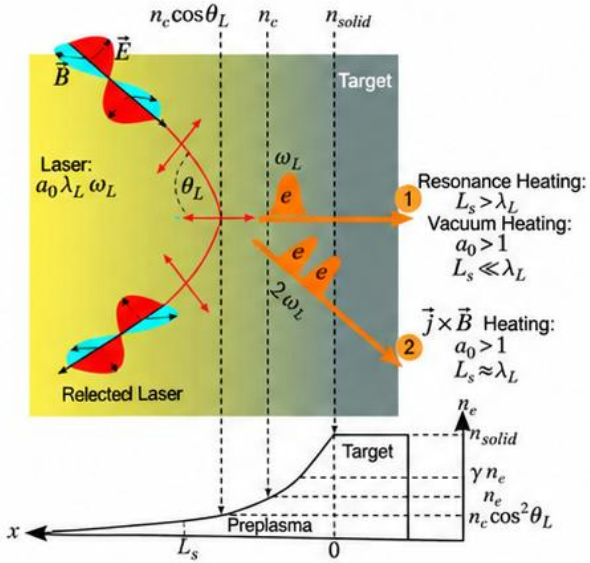
Low-density targets enhances electron heating (…but also ultrathin, mass limited etc.)

Bin, J. H., et al. *Phys. Rev. Lett.* 120.7 (2018): 074801.

Wilks, S. C., Kruer, W. L., Tabak, M., Langdon, A. B. "Absorption of ultra-intense laser pulses" Phys. Rev. Lett. 69, 1383 (1992).

Comparison of Electron Acceleration Mechanisms

Directionality / Bunching Period



Energetic Electron Generation and Transport in Intense Laser-Solid Interactions | SpringerLink

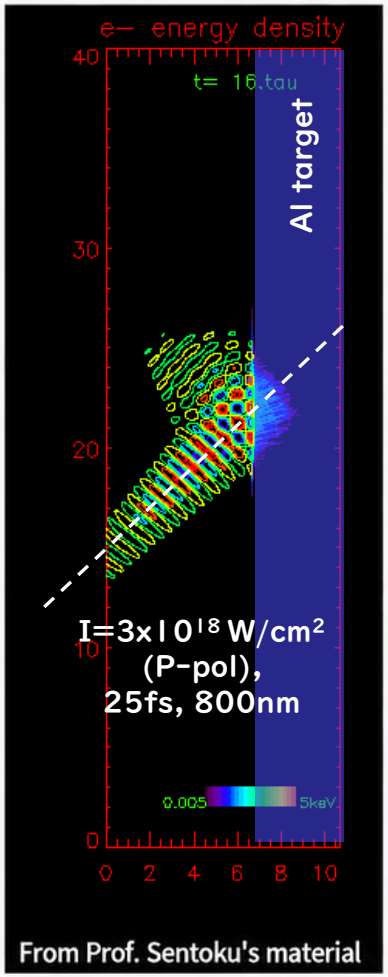
Resonance absorption / vacuum heating

⇒ target normal direction

J×B heating

⇒ laser-axis direction

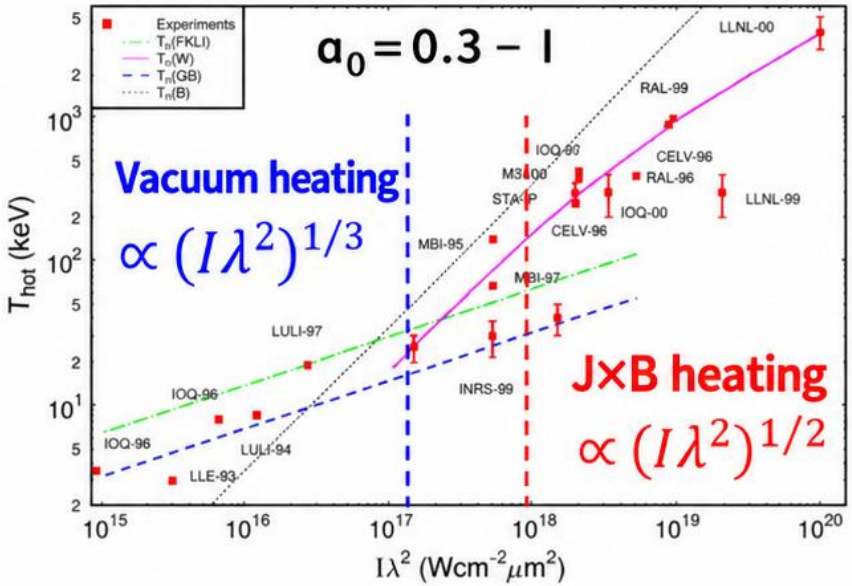
Interaction of a High-Intensity Laser with Solid (Al)



From Prof. Sentoku's material

Laser Intensity vs Electron Energy

(Fig. 5.19 from Gibbon)



$$T_h^{\mathrm{GB}} \simeq 7\left(I_{16}\lambda^2\right)^{1/3}, \qquad \text{Vacuum heating} \qquad (5.85)$$

$$T_h^{\mathrm{W}} \simeq mc^2(\gamma - 1)$$
$$= mc^2\left[\left(1 + \frac{p_{os}^2}{m^2c^2}\right)^{1/2} - 1\right] \qquad \text{J×B heating}$$
$$\simeq 511\left[\left(1 + 0.73 I_{18}\lambda_\mu^2\right)^{1/2} - 1\right] \text{ keV}. \qquad (5.86)$$

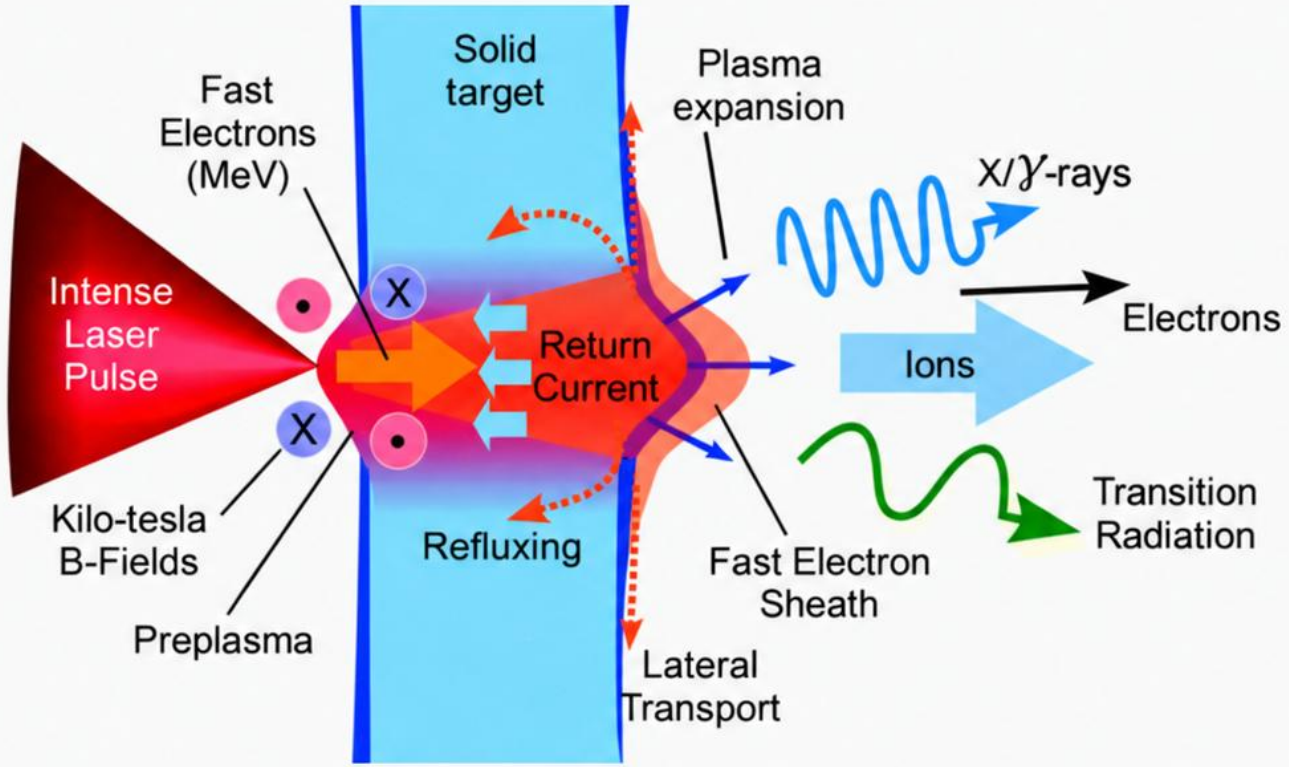
Section 4

Fast-Electron Transport and Sheath Formation

Transport of High-Density Electron Current in a Target

The current density of fast electron beams produced by J×B acceleration is typically 10^{12}–10^{13} A/m^2

If 1 J of laser light is converted into a fast electron beam with an efficiency of 5%,
the current reaches **5 MA** (100 fs, 100 keV, 25 μm diameter)



POINT

Energetic Electron Generation and Transport in Intense Laser–Solid Interactions | SpringerLink

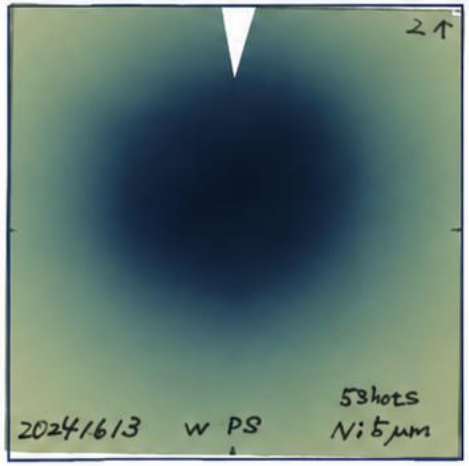
For such a high-density electron beam, **collective effects of electrons** (behavior as a current) dominate over single-particle effects.

Impact of Rear-Side Transport of Fast Electron Beams on Ion Acceleration

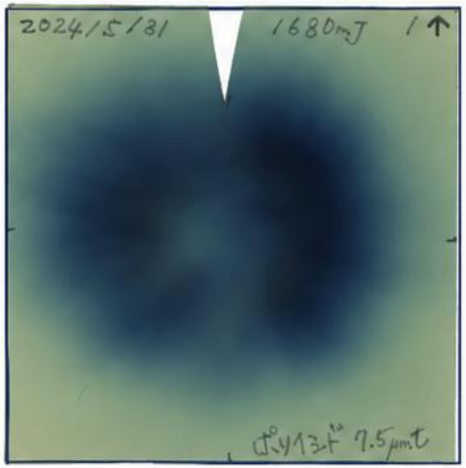
Item	Conductor	Insulator
Collisional scattering	Large ×	Small ○
Self-generated magnetic field	○ Neutralized (return current ◎) → Weak magnetic field	× No return current → Strong magnetic field / filamentation
Resistive electric field	ρ (small) → Resistive electric field ○	ρ (large) → Resistive electric field ×

$$\frac{\rho R_{\mathrm{Ni}}}{\rho R_{\mathrm{PI}}} \approx 4.2$$

Nickel has about 4 times larger ρR than polyimide



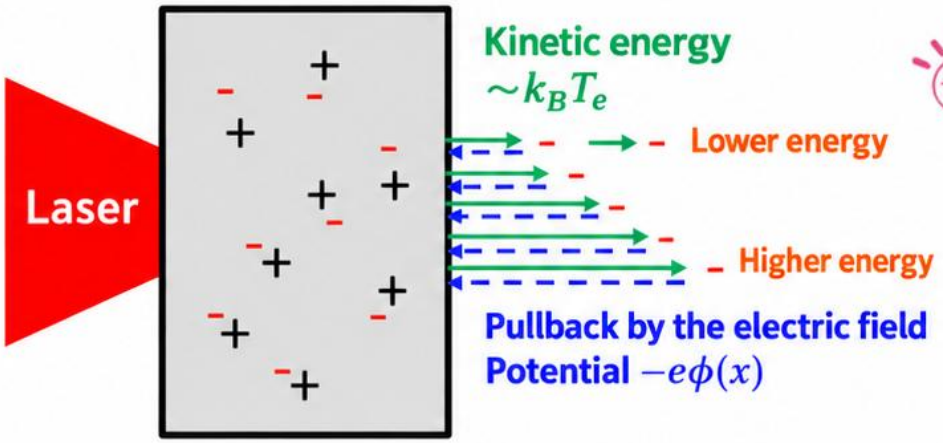
Ni 5 μm (conductor)



Polyimide 7.5 μm (insulator)

Formation of the Sheath Field at the Rear Surface of the Target

How strong and how long is the sheath field generated?



POINT

Electrons fly out until the outward force $k_B T_e$ and the pullback force $-e\phi(x)$ balance

The density distribution of fast electrons that reach the rear surface of the target can be approximated by a **Boltzmann distribution**:
(How are particles distributed by the potential $\phi(z)$?)

$$n_e(z) = n_{e0} \exp\left(\frac{e\phi(z)}{k_B T_e}\right),$$

Poisson equation
(What kind of potential $\phi(z)$ is generated by the particle distribution?)

$$\frac{d^2\phi}{dz^2} = -\frac{e\, n_e(z)}{\varepsilon_0}$$

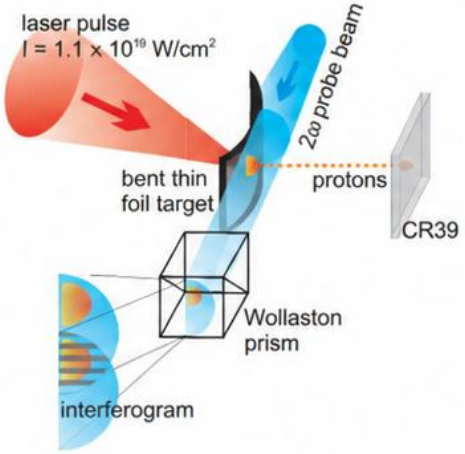
$$\frac{d^2\phi}{dz^2} = -\frac{e}{\varepsilon_0}\left(n_0 - n_0\, e^{e\phi/k_B T_e}\right) = \frac{n_0 e^2}{\varepsilon_0 k_B T_e}\phi \quad \text{(linearized)},$$

$$\frac{d^2\phi}{dz^2} = \frac{\phi}{\lambda_D^2}, \qquad \lambda_D \equiv \sqrt{\frac{\varepsilon_0 k_B T_e}{n_0 e^2}}.$$

Here $\exp(e\phi/k_B T_e) \approx 1 + \frac{e\phi}{k_B T_e}$ $(|e\phi| \ll k_B T_e)$ is used.

The sheath field decays exponentially over the Debye length
(typically 100 nm – 1 μm)

O Jäckel et al 2010 New J. Phys. 12 103027



- 10 TW Ti:sapphire (500 mJ, 80 fs, 800 nm)
- Focused intensity ~1.1 × 10^{19} W/cm^2
- Target: 6 μm-thick titanium foil

The spatial distribution of fast electrons reaching the rear surface was measured by optical interferometry.

The density distribution of fast electrons reaching the rear surface can be approximated by a Boltzmann distribution:

$$n_e(z) = n_{e0} \exp\left(\frac{e\phi(z)}{k_B T_e}\right), \qquad \frac{d^2\phi}{dz^2} = -\frac{e\, n_e(z)}{\varepsilon_0}$$

Figure 1. Schematic overview of the experimental setup.

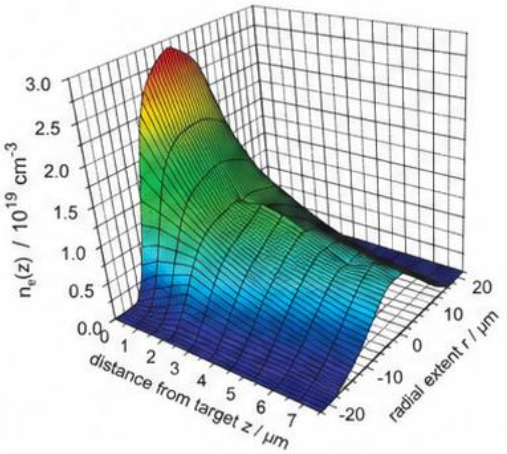


Figure 2. Electron density distribution of the electron sheath at the rear surface of the target foil recorded at a time step t_0.

Initial electron distribution on the ~100 fs timescale immediately after the onset of acceleration.

By solving the Poisson equation + Boltzmann distribution for n_e, we obtain the 1D Poisson–Boltzmann solution.

$$n_e(z>0) = n_{e0} \exp\left\{-2\ln\left(1+\frac{z}{\sqrt{2e}\,\lambda_D}\right) - 1\right\}$$

As predicted by this equation, the electron density distribution **decays exponentially**.

POINT

When the experimental results are fitted with the above function:

Electron density $n_{e0} \approx 8.4 \times 10^{19}$ cm^{-3} (0.1 n_c)
Debye length $\lambda_D = 1.0 \pm 0.2$ μm
Electron temperature $k_B T_e = 1.5 \pm 0.4$ MeV
The lateral distribution is Gaussian (FWHM ≈ 21 μm)
About 4–5 times the laser focal spot diameter.

O Jäckel et al 2010 New J. Phys. 12 103027

The sheath electric field is the potential gradient at the rear surface (boundary) of the target

Here

$\phi(z)$: electrostatic potential

$z = 0$: rear surface position of the target
(the point where the boundary condition is imposed)

$$E(z) \equiv -\frac{d\phi}{dz}, \quad E_{\mathrm{TNSA}} \equiv E(z=0)$$

In other words, the sheath field is defined as the slope of the potential at the rear boundary.

When the density distribution of fast electrons follows the Poisson–Boltzmann solution

Equation for the sheath field

$$E_{\mathrm{TNSA}} = \sqrt{\frac{2}{e_N}}\sqrt{\frac{k_B T_e\, n_{e0}}{\varepsilon_0}}$$

$$T_e = 1.5\ \mathrm{MeV},$$

$$n_{e0} = 8.4 \times 10^{19}\ \mathrm{cm}^{-3}$$

Sheath field predicted at T = 0, z = 0 (target rear surface)

POINT

$$E_{\mathrm{TNSA}} = (1.1 \pm 0.4)\ \mathrm{TV/m}$$

TV/m-class sheath fields are generated even with compact high-intensity laser systems.

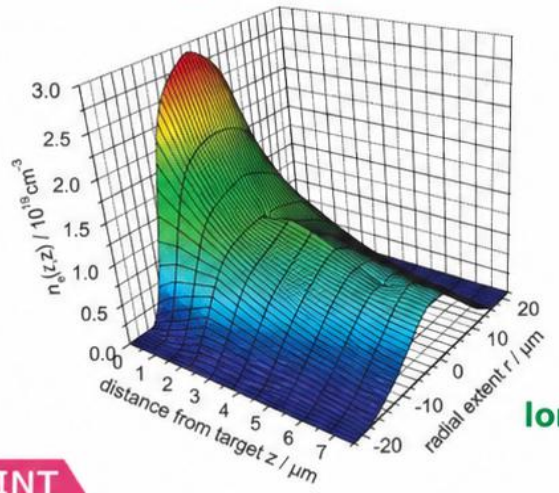
Section 5

Target Normal Sheath Acceleration (TNSA)

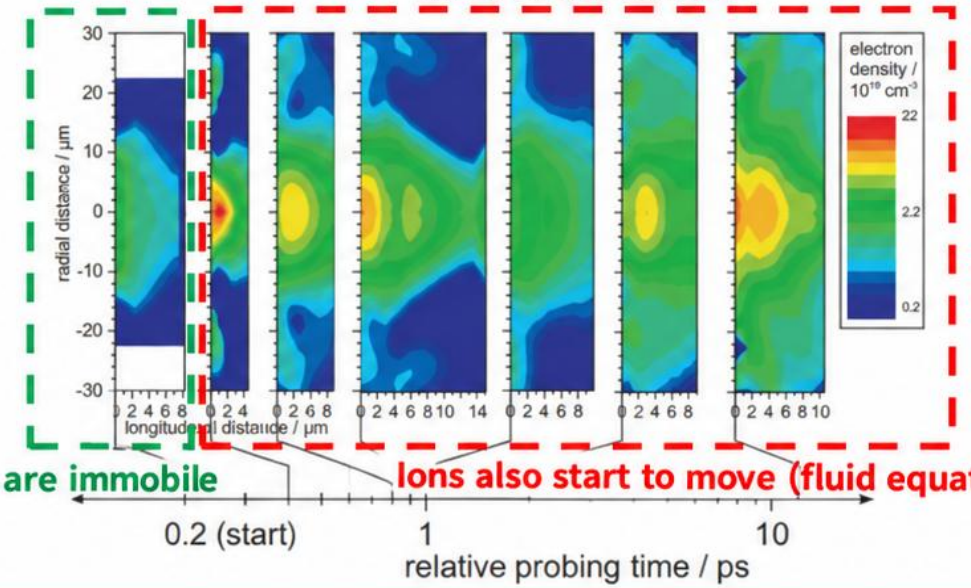
Time Evolution of Fast-Electron Transport and the Sheath Field

O Jäckel et al 2010 New J. Phys. 12 103027

Spatial distribution of fast electrons at the earliest stage (t = 0.2)



Time evolution of the spatial distribution of fast electrons



POINT

At the earliest stage (t = 0.2), the distribution is determined by the balance between the electron energy and the self-generated electric field.

After that (t > 0), electrons expand and spread significantly in space and time, so the initial static 1D solution can no longer describe the system correctly.

⇒ **Therefore, models in which the plasma expands into vacuum while accelerating ions are used:**

- **Isothermal expansion model** (Jean Mora, Phys. Rev. Lett. 90, 185002, 2003)
- **Adiabatic expansion model** (Murakami & Basko, Phys. Plasmas 13, 012105, 2006)

About the Isothermal Expansion Model (Mora 2003)

(a) Ion fluid equations

Continuity equation

$$\frac{\partial n_i(z,t)}{\partial t} + \frac{\partial}{\partial z}\left(n_i(z,t)\, v_i(z,t)\right) = 0$$

Equation of motion

$$\frac{\partial v_i(z,t)}{\partial t} + v_i(z,t)\,\frac{\partial v_i(z,t)}{\partial z} = -\frac{Ze}{m_i}\frac{\partial \phi(z,t)}{\partial z}$$

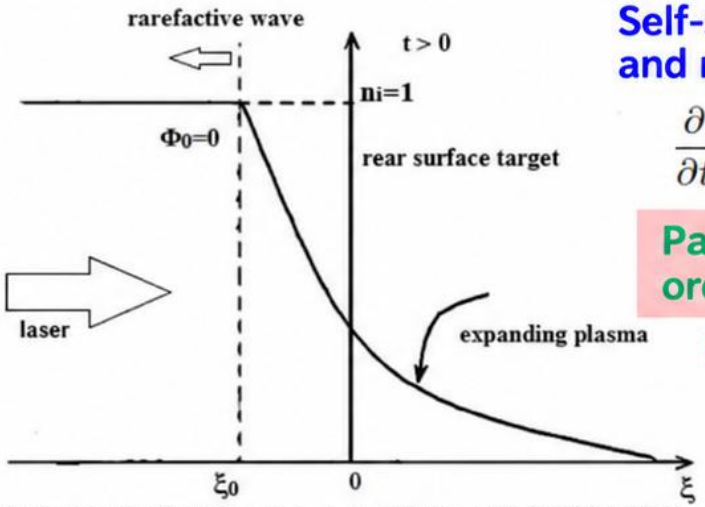
Sheath field

(b) Electron distribution (Boltzmann distribution)

$$n_e(z,t) = n_{e0}\exp\left(\frac{e\,\phi(z,t)}{k_B T_e}\right)$$

(c) Poisson equation

$$\frac{\partial^2 \phi(z,t)}{\partial z^2} = -\frac{e}{\varepsilon_0}\left(Z n_i(z,t) - n_e(z,t)\right)$$



D. Bennaceur-Doumaz et al., J. Appl. Phys. 117, 043303 (2015)

Self-similar transformation and nondimensionalization

$$\eta \equiv \frac{z}{c_s t}, \qquad c_s = \sqrt{\frac{Z k_B T_e}{m_i}}$$

Sound speed

$$\frac{\partial}{\partial t} = -\frac{\eta}{t}\frac{d}{d\eta}, \qquad \frac{\partial}{\partial z} = \frac{1}{c_s t}\frac{d}{d\eta}.$$

Because the expansion is isothermal, the sound speed is constant.

Partial differential equations → transformed into ordinary differential equations, making them easier to solve.

Final expressions that predict:

Velocity of the ion expansion front

$$\frac{v_f(t)}{c_s} = 2\,\mathrm{asinh}\left(\frac{t}{\tau}\right) = 2\,\ln\left(\frac{t}{\tau} + \sqrt{1+\left(\frac{t}{\tau}\right)^2}\right).$$

POINT

Maximum ion energy can be predicted as

$$E_{\max}(t) = \tfrac{1}{2} m_i v_f^2 = 2\,Z\,k_B T_e \left[\ln\left(\frac{t}{\tau} + \sqrt{1+\left(\frac{t}{\tau}\right)^2}\right)\right]^2.$$

Time evolution of fast-electron transport and the sheath field

Isothermal Expansion Model (Mora 2003)

- Assumption: electron temperature T_e=const.
- Result: the maximum ion energy

$$E_{\max}(t) \approx 2T_e \left[\ln\left(\tau_{\mathrm{acc}} + \sqrt{1+\tau_{\mathrm{acc}}^2}\right)\right]^2$$

∗ Continues to increase indefinitely with time.

⇒ In practice, a finite-time cutoff is required; an external end time of acceleration must be introduced.

- Example: in Fuchs 2006,
  "acceleration time $\tau_{\mathrm{acc}} \approx 1.3\,\tau_{\mathrm{L}}$ (τ_{L}: laser pulse duration)" is empirically limited.

Adiabatic Expansion Model (Murakami & Basko 2006, etc.)

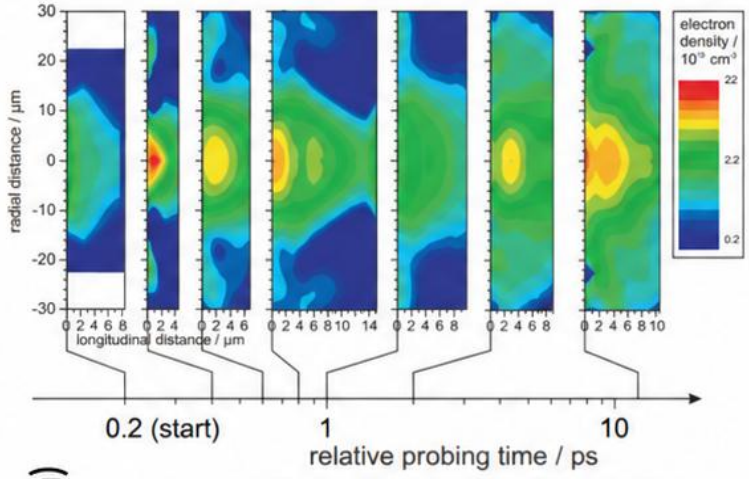
- Assumption: electrons are not supplied with energy externally and cool adiabatically.
- Temperature: $T_e(t) \propto t^{-\alpha}$ $(\alpha \sim 1-2)$. • Result: the electric field also decays as $E(t) \propto n_e T_e$.

$$E_{\max} \simeq \varepsilon_0\, W\left(\frac{\Lambda^2}{2}\right)$$

⇒ Therefore, ion energy naturally saturates with time.

- $W(x)$: Lambert W function
- $\varepsilon_0 \approx \frac{2Zk_BT_{e0}}{\nu(\gamma-1)}$
  - T_{e0} : initial electron temperature
  - Z : ion charge
  - γ : adiabatic index (non-relativistic 5/3, relativistic 4/3)
  - ν : geometrical dimension (planar 1, cylindrical 2, spherical 3)
- Λ : dimensionless expansion parameter (determined by e–i density ratio and expansion time)

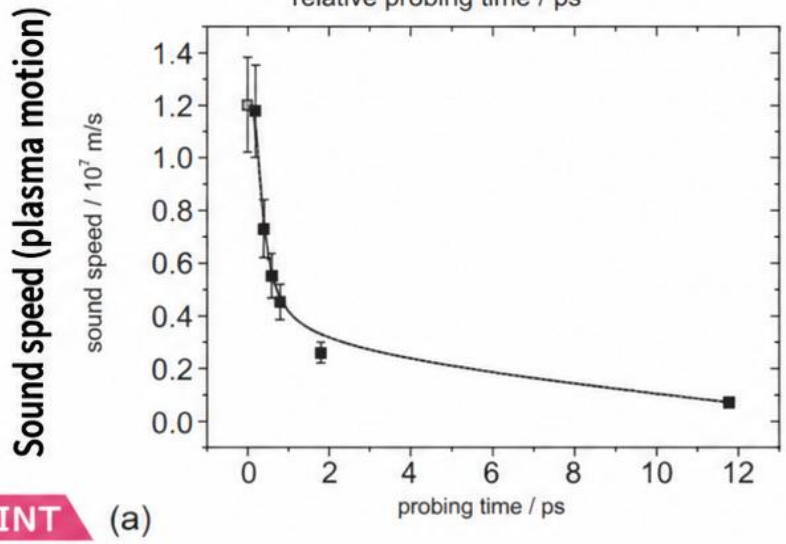
O Jäckel et al 2010 New J. Phys. 12 103027

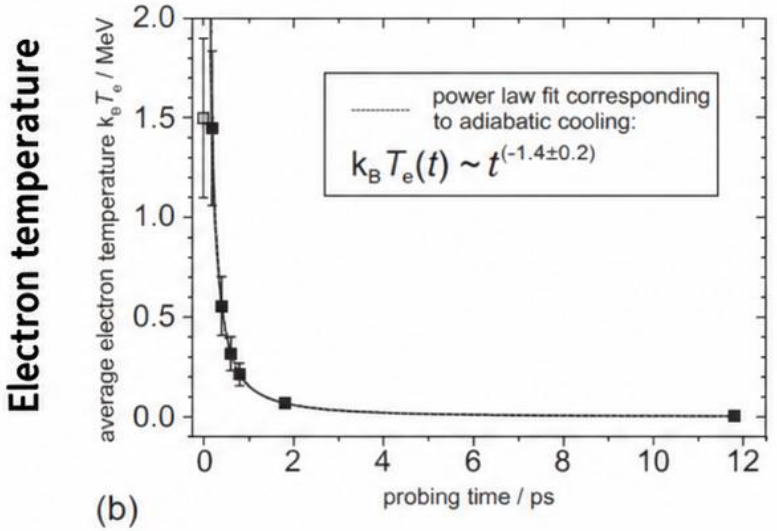


From the time evolution of constant-density contours,

$$\dot{z}(t, n_e = \text{const}) = c_s(t) = \sqrt{\frac{Z\, k_B T_e(t)}{m_i}}$$

assuming the motion of the observed contour represents plasma expansion,
the observed contour velocity was taken as the sound speed $c_s(t)$, and $T_e(t)$ was determined.

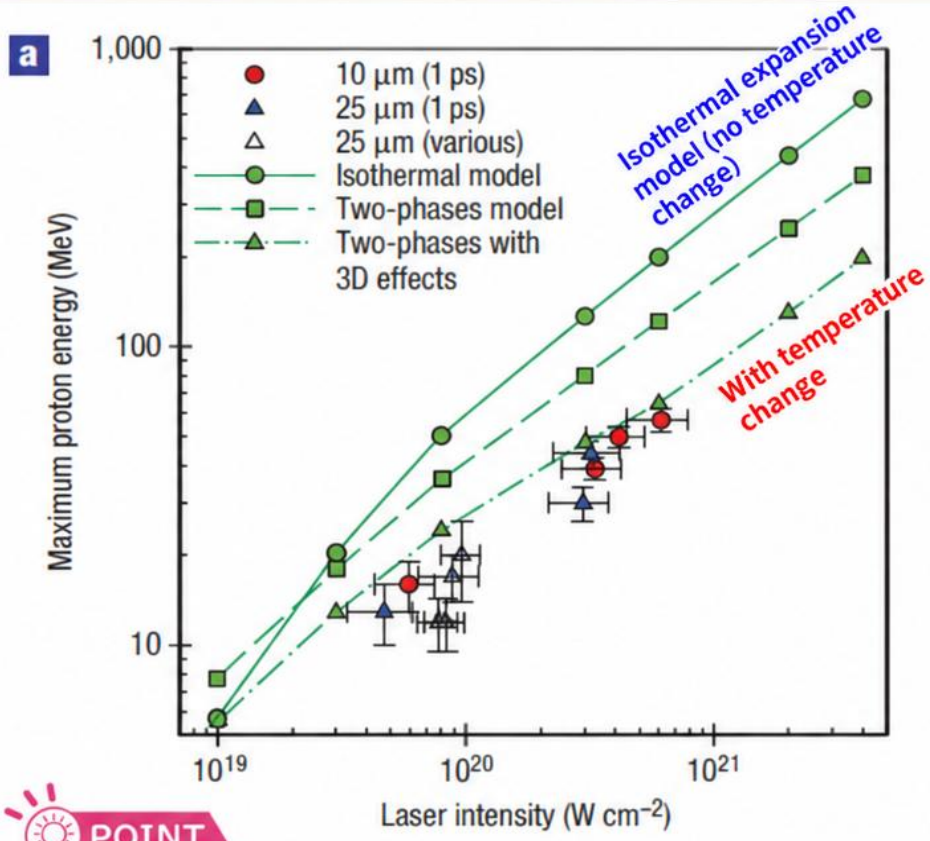




POINT

The **adiabatic expansion model**, in which $T_e(t) \sim t^{-1.4}$ decreases with time, reproduces the data well.

Characteristics of Ion Beams Accelerated by TNSA



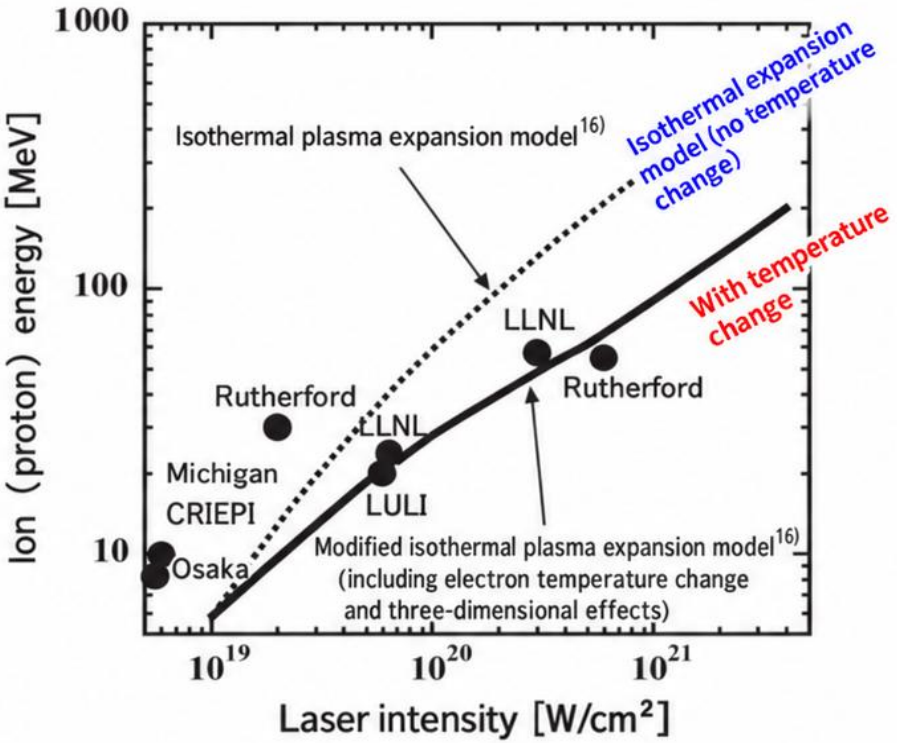


Fig. 3 Scaling of laser-ion acceleration (in the isothermal expansion regime). Scaling of the maximum ion (proton) energy in the isothermal plasma expansion scheme as a function of laser intensity. In the high-intensity region, where the effect of electron temperature change and three-dimensional effects are taken into account, the modified isothermal plasma expansion model agrees well with experimental results[16)]. Note that the scaling does not take into account the effect of the laser wavelength.

POINT

Predictions from the isothermal expansion model tend to overestimate the maximum energy compared with experimental values.

⇒ **Therefore, effects such as temperature decrease and three-dimensional electron transport should be included.**

Ranking of Maximum Energy of Laser-Driven Ion Beams

QST

Rank	Maximum energy	Year / Facility	Laser system	Reference
1	**150 MeV** (+15 / −11 MeV)	**2024** **HZDR** (Germany)	**DRACO-PW** **22.4 J / 30 fs** **Ti:Sa**	T. Ziegler et al., *Nature Physics* 20, 1211 (2024)
2	**132 MeV**	**2026** **Osaka University** **ILE / LFEX** (Japan)	**~ 10 kJ / 1.5 ps** **Nd:glass**	T. Minami et al., *Prog. Theor. Exp. Phys.* 2026, 103J01 (2026)
3	**> 110 MeV**	**2025** **CoReLS** (Korea)	**4 PW** **Ti:Sa**	Y. Shou et al., *Nature Communications* 16, 1487 (2025)
4	**> 94 MeV**	**2018** Rutherford Appleton Laboratory (UK)	**Astra Gemini** **0.5 PW Ti:Sa**	A. Higginson et al., *Nature Communications* 9, 724 (2018) (highest energy between 94 and 101 MeV)
5	**93 MeV**	**2016** **CoReLS** (Korea)	**Ti:Sa** **30 fs**	I. J. Kim et al., *Physics of Plasmas* 23, 070701 (2016)

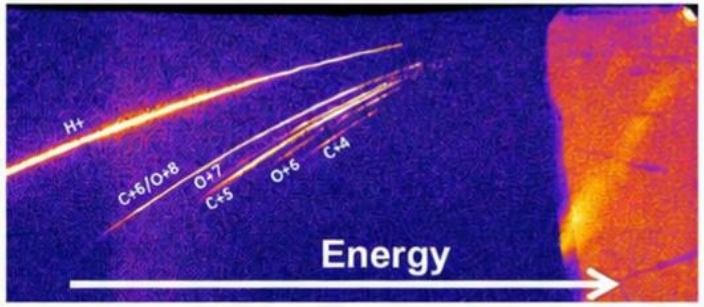
At ELI-NP (Romania), ELI Beamlines (Czech Republic), Apollon (France), and SULF (China),
10 PW-class lasers are currently under development or have started operation.

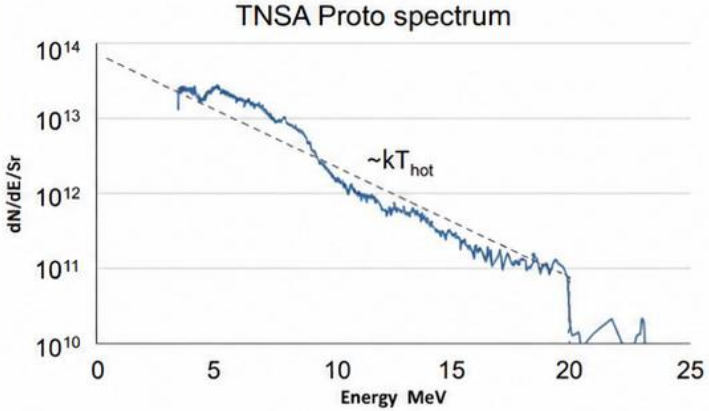
⇒ With laser acceleration alone, **proton energies have experimentally reached 150 MeV**, and are expected to extend **beyond 200 MeV** with multi-PW and 10-PW-class lasers, opening the possibility of future applications such as **ion-beam cancer therapy**.

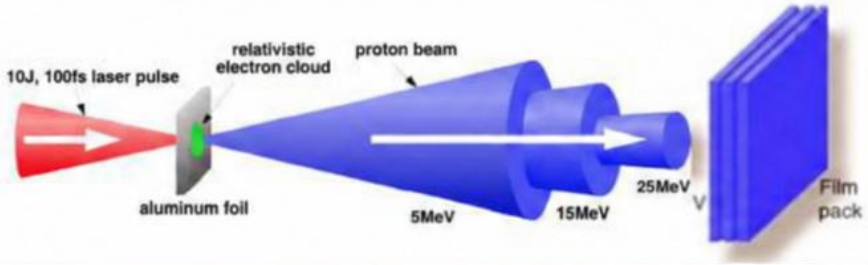
Characteristics of Ion Beams Accelerated by TNSA

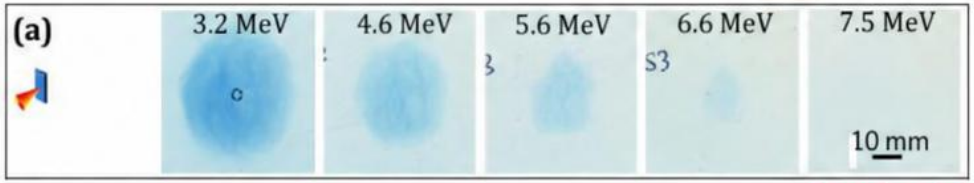
POINT

- Acceleration distance ~ several tens of μm
- Accelerating field ~ 10^{12} V/m
- Multiple ion species, broad energy spectrum
- Short pulse duration (< 100 ps)
- Divergent beam (several tens of degrees)
- Low emittance 0.1 π mm·mrad @ > 15 MeV
- High brightness 10^{11}–10^{13} protons (ions) per shot

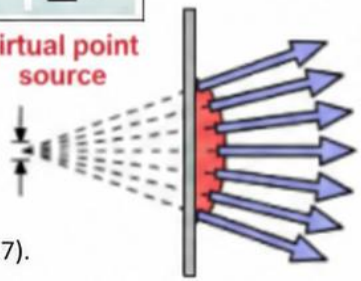




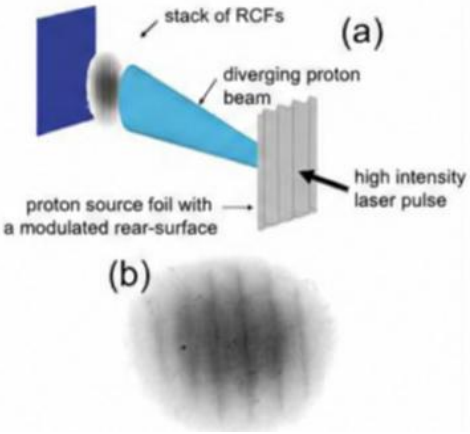




S. Kar et al., Nat. Com. 7, 10792 (2016)



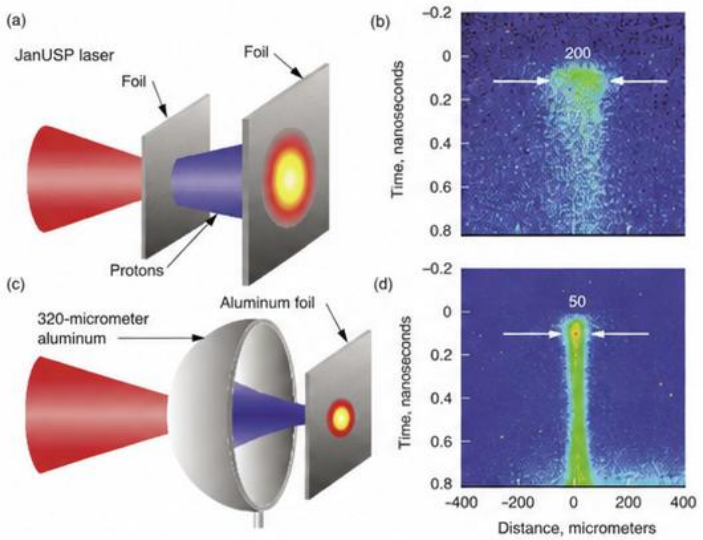
Laminar source



Emittance growth mechanisms for laser-accelerated proton beams, Kemp, A., Fuchs, J., Sentoku, Y., Sotnikov, V., & Bakeman, M., PRE (2007).

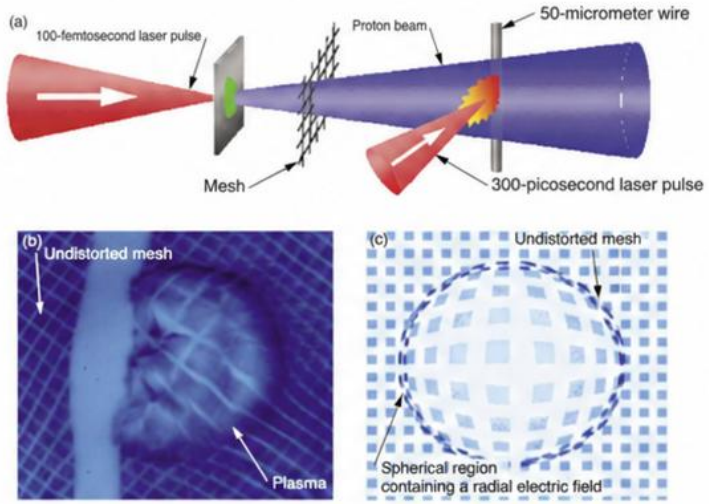
Applications of Ion Beams Accelerated by TNSA ①

Isochoric heating by proton beams
(instantaneous heating before the plasma expands)



(a) Layout for the proton-beam experiments using the Janus ultrashort-pulse (JanUSP) laser. When JanUSP irradiates an aluminum foil, it creates a proton beam that then heats a second foil. Both foils are 10 micrometers thick, and the second foil is placed 250 micrometers behind the first. (b) The plasma created in the second foil is almost 200 micrometers in diameter. (c) Layout for the experiments with a curved target. (d) When the target's rear surface is curved, the laser produces a focused proton beam that is 50 micrometers in diameter and almost 10 times more powerful than the beam produced with a flat target.

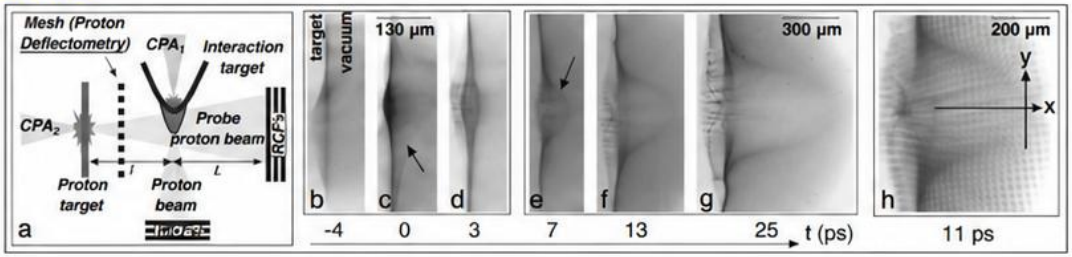
Proton radiography of electromagnetic fields



(a) Another particle-deflection technique uses a single grid to subdivide protons into hundreds of small proton beamlets. (b) Proton radiograph of plasma created by a 300-picosecond laser pulse on a 125-micrometer-thick wire shows the plasma magnified and distorted because of the plasma's electric and magnetic fields. The pattern is similar to (c) a hybrid code simulation of protons propagating through a spherical region that contains a radial electric field, which reproduces the essential features of the experiment.

https://str.llnl.gov/str/December03/Patel.html

Proton radiography of electromagnetic fields
Time-resolved measurements using TOF



L. Romagnani et al., PRL **95,** 195001 (2005)

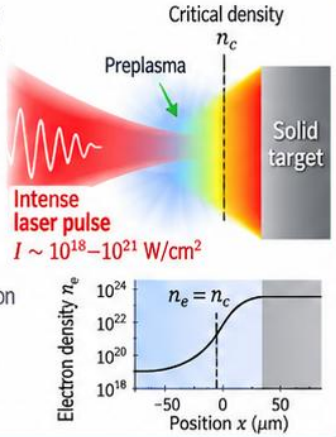
Section 6

Summary

Key Takeaways

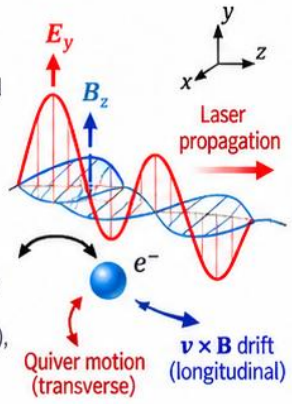
1 Laser–Plasma Interaction (Slides 3-5)

- Ultrashort, high-intensity laser creates a preplasma at the target surface.
- Laser propagates up to the critical density n_c where the refractive index approaches zero.
- Steep density gradient enables efficient energy absorption and hot-electron generation.



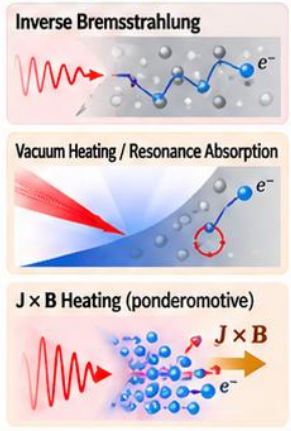
2 Relativistic Electron Motion (Slides 6-12)

- In an intense laser field, electrons oscillate relativistically with normalized vector potential $a_0 = eE_0/m_e c\omega \gtrsim 1$.
- Quiver motion is mainly transverse, with a $\boldsymbol{v} \times \boldsymbol{B}$ drift in the propagation direction.
- A single electron in a plane wave cannot gain net energy (infinite plane wave), so energy absorption requires plasma effects.



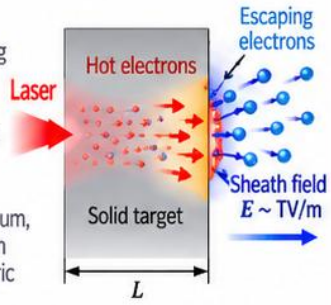
3 Laser Energy Absorption and Fast-Electron Generation (Slides 13-22)

- Laser energy is absorbed in plasmas via multiple mechanisms depending on density, intensity, polarization, and incidence angle.
- These processes generate hot electrons with temperatures of ~ 0.1–10 MeV, which drive subsequent ion acceleration.



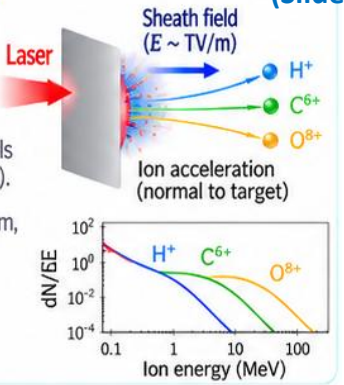
4 Fast-Electron Transport and Sheath Formation (Slides 23-28)

- Hot electrons propagate through the target, forming a return current and generating self-magnetic and resistive electric fields.
- At the rear surface, hot electrons escape into vacuum, creating charge separation and a strong sheath electric field (TV/m).



5 Target Normal Sheath Acceleration (TNSA) (Slides 29-37)

- The rear-surface sheath field accelerates ions normal to the target.
- Ion energies follow plasma expansion models (isothermal or adiabatic).
- Produces broad-spectrum, quasi-exponential ion beams with multi-MeV protons and higher-charge-state ions.



POINT Laser-driven ion acceleration uses ultra-strong plasma fields to accelerate ions over short distances, offering new possibilities for compact accelerators.